Theoretical Heat Pump Ground Coil Analysis with Variable Ground Farfield Boundary Conditions

V. C. Mei
Energy Division
Oak Ridge National Laboratory
Oak Ridge, TN 37831

Heat pumps have long been recognized for their energy conservation potential. Low-grade heat from air, a convenient body of water, or the ground can be used as the heat source, or sink, for heat pump operation. Ground-coupled heat pumps can greatly improve the overall system's performance because of stable, year-round ground temperatures, the replacement of the outdoor fan with a small fluid-circulating pump, and the elimination of outdoor coil frost and defrost losses.

There are several major difficulties encountered in a detailed analysis of ground coil performance:

1. Lack of knowledge of soil thermal conductivity and diffusivity, both highly dependent on the soil moisture content in a given location.
2. Moisture migration caused by the temperature gradient.
3. Ice formation around the coil, with attendant release of latent heat and a step change in thermal properties in the soil frozen region.
4. The effect of seasonal temperature variation at depths below the ground surface.
5. Possible thermal resistance due to lack of intimate contact of the coil with soil.
6. The effect of ground coil size and material.
7. The effect of coil cyclic operation.

When the ground coil is designed mainly for winter heating purposes, soil moisture will migrate toward the surface, which causes the soil layer close to the surface to be saturated, or nearly saturated, with moisture. Therefore, the ground thermal properties are very stable in the winter. Moisture migration in coil winter operation thus has only a very minor effect on coil operation. Also, because any gaps between coil and soil will be filled with moisture caused by the moisture migration toward the coil in the winter, no contact resistance will be encountered. Field experimental results (Coogan, 1949) indicate that the latent heat released by the soil moisture freezing is small compared with the total energy absorbed by the coil. If we concentrate our analysis on winter operation, difficulties 1, 2, 3, and 5 can be neglected. The remaining difficulties still represent a very complicated problem, however.

The most popular current theoretical approach utilizes line source (or cylindrical source) theory (Ingersoll et al., 1950). The major drawbacks of this approach are:

1. One has to assume, or guess, the strength of the line source, which makes this approach more dependent on empirical data.
2. The coil fluid-wall convective heat transfer resistance is generally ignored even when the fluid flow is in the laminar region.
3. The continuous coil fluid temperature change indicates that the strength of the line source will not be constant along the coil.
4. The effect of the seasonal temperature variation at depths is generally ignored so that the problem can be treated as radially symmetrical.

In this paper, a three-dimensional mathematical model is developed to describe ground coil operation. The model considers the fluid flow inside the coil, coil material and size, and cyclic operation of the coil. The farfield conditions are specified with the empirical equation derived by Kusuda and Achenbach (1965) so that they are a function of depth and time of the year.

Mathematical Model

The model is based on energy balances subject to the following assumptions:

1. The soil is homogeneous
2. The soil thermal properties are constant
3. The fluid temperature and velocity are uniform at any coil cross section
4. The coil is buried deep enough that the distance between ground surface and coil can be considered as farfield

5. Only a single coil is in the ground
6. Heat transfer up to the coil wall is axially symmetrical.

For winter operation, assumptions 1 and 2 are close to the real ground conditions because the ground top layer is saturated with moisture. Assumption 3 is valid for large coil length-to-diameter ratio. Field experiments by Freund and Whitlow (1959) indicated that thermal penetration caused by the coil was not more than 1 m. Since coils are usually buried at least that deep, assumption 4 is also valid. The coils are usually buried at least 2 m apart so that thermal interference will not occur, and a single coil analysis is adequate for the system, which justifies assumption 5. Because the ground coil outside diameter is usually not more than 5 cm, and the coil wall is no more than 0.32 cm thick, assumption 6 will cause a very small error in calculating ground temperature distribution.

With the above assumptions, the following operations can be derived for the system shown in Figure 1.

Heat exchange between the fluid and coil inside wall:

$$-V\frac{\partial T_f}{\partial x} + \frac{2K_p}{r_0\rho_f C_f}\frac{\partial T_p}{\partial r}\bigg|_{r_0} = \frac{\partial T_f}{\partial t} \tag{1}$$

Heat transfer in the coil wall:

$$\frac{\partial T_p}{\partial r^2} + \frac{1}{r}\frac{\partial T_p}{\partial r} = \frac{1}{\alpha_p}\frac{\partial T_p}{\partial t} \quad (r_0 \le r \le r_1). \tag{2}$$

Heat transfer in the soil:

$$\frac{\partial^2 T_s}{\partial r^2} + \frac{1}{r}\frac{\partial T_s}{\partial r} + \frac{1}{r^2}\frac{\partial^2 T_s}{\partial \theta^2} = \frac{1}{\alpha_s}\frac{\partial T_s}{\partial t} \tag{3}$$

where heat transfer in the x direction in Eqs. 2 and 3 is neglected because of low thermal conductivity values of plastic coil and soil and long distance in the x direction.

Boundary conditions:

At $r = r_0$,

$$h(T_p - T_f)\bigg|_{r_0} = K_p\frac{\partial T_p}{\partial r}\bigg|_{r_0}. \tag{4}$$

At $r = r_1$, in winter:

$$T_s = T_p. \tag{5}$$

At $r = r_1$, other condition:

$$2\pi K_p\frac{\partial T_p}{\partial r}\bigg|_{r_1} = K_s\int_0^{2\pi}\frac{\partial T_s}{\partial r}\bigg|_{r_1} d\theta. \tag{6}$$

At $r = r_F$,

$$T_{sF} = TA - DT \times \exp\left(-Z\sqrt{\frac{\pi}{8766\alpha_s}}\right) \times \cos\left(\frac{2\pi t_0}{8766} - \phi - Z\sqrt{\frac{\pi}{8766\alpha_s}}\right) \tag{7}$$

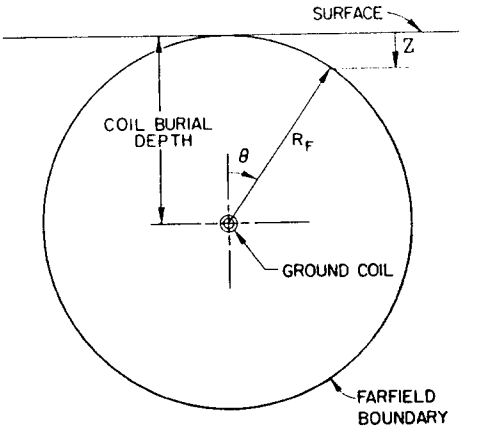

Figure 1. Diagram of ground coil.

Equation 5 is acceptable for coil winter operation, for no contact resistance. T_s is then independent of θ at the pipe wall. Equation 7 is the correlation of Kusuda and Achenbach (1965) and ϕ is the phase angle of the earth temperature cycle, below grade, in radians.

Initial conditions ($t = 0$):

$$T_f = T_{fi}(x)$$
$$T_p = T_{pi}(x, r)$$
$$T_s = T_{si}(x, r) \tag{8}$$

where T_{fi}, T_{pi}, and T_{si} are known functions of x and r. For the coil to start operating, T_{fi}, T_{pi}, and T_{si} can easily be calculated by Eq. 7.

Fluid inlet condition:

$$T_f(t, x = 0) = T_{f0}(t) \tag{9}$$

$T_{f0}(t)$ is a known function of time t that represents the heat pump operation. For a given heat pump, if we know the fluid inlet temperature and flow rate to the fluid-refrigerant heat exchanger, the fluid exit temperature can easily be calculated from the manufacturer's published heat pump performance data. The heat pump exit fluid represents the ground coil inlet fluid.

The model described so far is for the ground coil with fluid circulation. During the "off" cycle period, the fluid velocity V in Eq. 1 is zero. Since the fluid thermal capacity is very small, Eq. 4 can be written in the form:

$$T_f = T_p. \tag{10}$$

Computer Simulation and Discussion

A finite-difference scheme computer code was written to solve the mathematical model for both continuous and cyclic operations. The computer program uses an explicit solution of a finite-difference approximation to this system of equations to calculate the temperature at fixed nodal points in the fluid, pipe, and ground. A fixed longitudinal spacing of nodes is used, an

unequal radial spacing of nodes in the ground is permitted, and an equal circumferential spacing in terms of angle is used in the ground. Two time steps are involved: the first is quite small and is used for stability of the coil wall and fluid region; the second, which is substantially larger, is used in the soil region.

The model was used to simulate the field test results provided by Brookhaven National Laboratory (Metz, 1983). The fluid and ground temperatures were provided as daily averages along with the heat pump total "on" time, daily energy absorbed from the ground, and average daily coil flow rates.

Properties of the coil, soil, and fluid follow:

Coil length, 152.5 m
Coil burial depth, 1.2 m
Coil size, 4.09 cm ID, 4.63 cm OD
Coil material, medium-density polyethylene
Coil thermal conductivity, 0.46 W/m · °C
Coil specific heat, 2,174 J/kg · °C
Fluid, water-ethylene glycol (20 wt. %) mixture
Soil, sandy with 10 vol. % moisture content
Soil thermal conductivity, 1.731 W/m · °C
Soil thermal diffusivity, 0.0036 m^2/h
Flow rate 0.927 m^3/h avg. during "on" time
Yearly avg. temp. TA, 10.232°C
Amplitude of yearly temperature variation DT, 12.759°C
Phase angle, ϕ, 0.352 radian

The thermal properties of the fluid were taken from the *ASHRAE Handbook* (1981). The farfield temperature was allowed to vary as indicated by Eq. 7. The ground coil inlet fluid temperature from the test data was input to the computer code.

Flow was typically in the transition region, with N_{Re} from 2,500 to 3,500. Available correlations for flow in this region (Jacob, 1958; Donne and Bowditch, 1963; VDI-Warmeatlas, 1977) led to a minimum N_{Nu} of 25, with values in the range 25 to 55. Computer results were independent of N_{Nu} in the range, and $N_{Nu} = 55$ was used for the calculation shown here.

Forty-four days were simulated, starting on day number 329 (November 26, 1981), the day the heating season really began. Since only the fraction of "on" time per day was given in the experimental data, the computer code, which could handle the cyclic operation, was instructed to run the same fraction of "on" time per hour.

Figure 2 shows the simulation of the daily energy absorbed from the ground. Test results for the first nine days were misprinted due to a computer program error confirmed by Brookhaven and are not shown here. After the first nine days, the computer code predicted field experimental results very well. Figure 3 shows the simulation of the coil exit field temperature during the "off" cycle period. The computed temperatures were for the most part about 1°C higher than the test results. There are two reasonable explanations:

1. The boundary condition when fluid is stopped, Eq. 10, is lifting the fluid temperature to equal the coil inside wall temperature, which is not true.

2. The exact cycling schedule was not given, which is an important factor in determining the fluid temperature.

Detailed analysis of boundary conditions when fluid flow stops involves natural convection in a long horizontal coil. Because the model predicts the daily energy absorption from the ground well, which is most important in designing the ground coil, further analysis of the heat transfer problem during the heat pump "off" cycle is not warranted for this study.

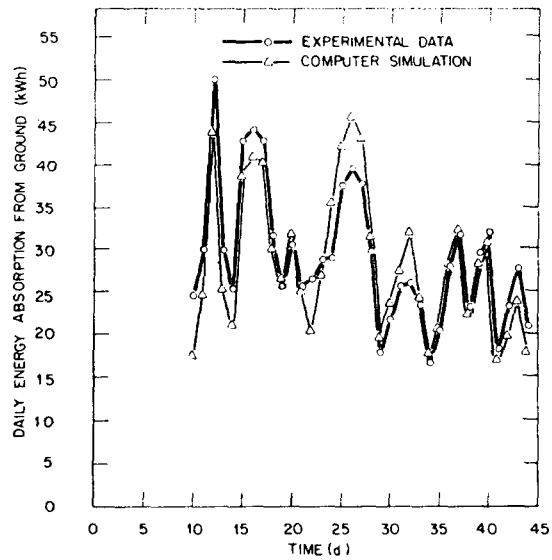

Figure 2. Simulation of daily energy absorption.

Figure 4 shows the calculated ground temperature distribution after 42 days' simulation. Although no experimental data are provided for comparison, the figure represents a very realistic ground temperature distribution because it is similar to those measured by Smith (1950) and Johnson et al. (1983).

Figure 5 shows the effect of ground coil wall thermal conductivity, K_p, for 15 days of continuous operation with a fluid inlet temperature of 0°C and the parameters of the Brookhaven

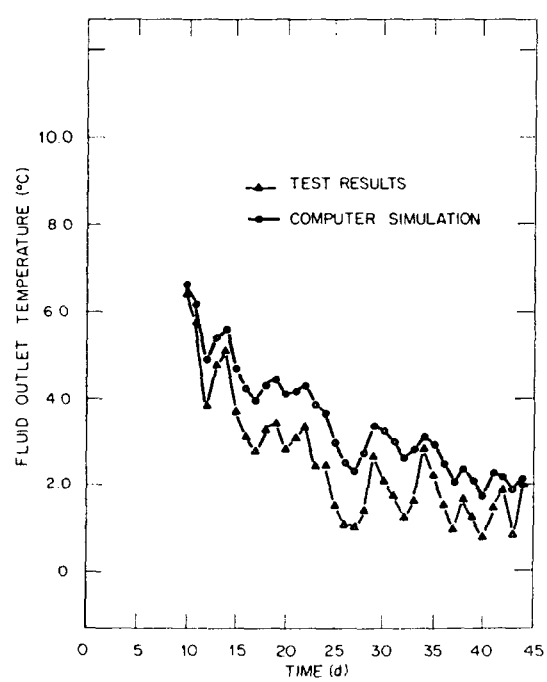

Figure 3. Simulation of ground coil fluid temperature at coil exit.

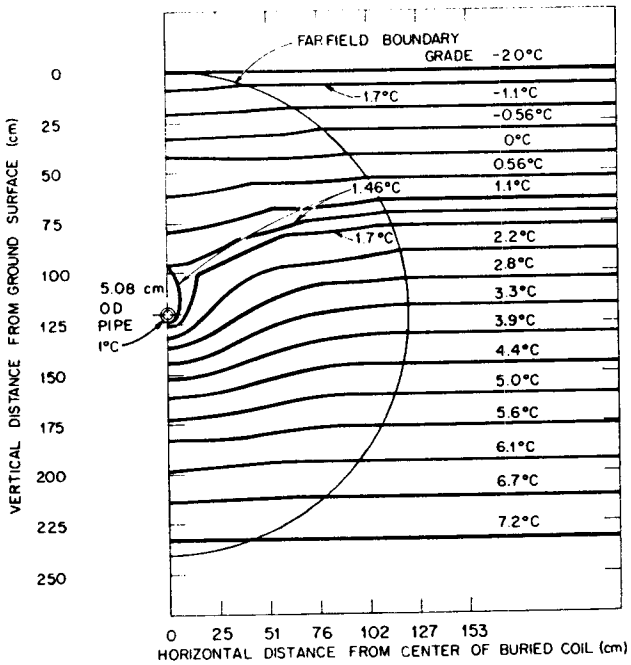

Figure 4. Calculated ground temperature distribution around coil.

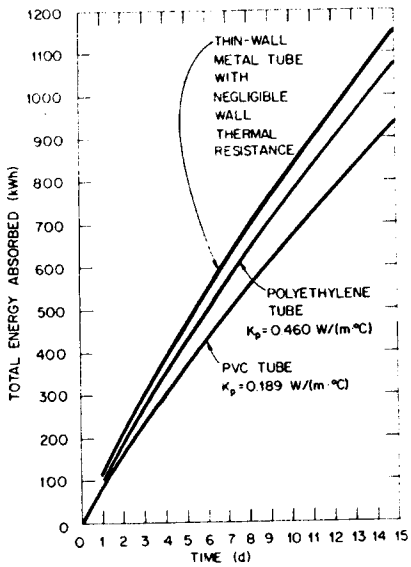

Figure 5. Effect of coil wall material on total energy absorption.

study. When K_p was reduced from 0.46 W/m · °C) (base case) to 0.189 W/m · °C (the thermal conductivity of polyvinyl chloride), the ground coil capacity was reduced by 12.3%. When thin-wall metal coil was assumed, the coil performance increased by 7.7%. Past experience indicated that copper coil joints, in addition to being more costly, are difficult to solder and often become a source of fluid leakage. The use of plastic tubing (polyethylene or polybutylene) as the ground coil has become common practice for several reasons: plastic tubing does not corrode; tube joints can be easily welded together (leakproof plastic welding is an important improvement over soldering metal joints); and plastic tubing is two to three times cheaper than copper tubing for the same tube size. Besides, the parametric study shows that using thin-wall metal tubing only increases the coil performance by 7.7% over polyethylene tubing after 15 days of continuous operation. The performance improvement is just not enough to offset the advantages of plastic tubing over metal.

Coil burial depth is a factor of concern. Theoretically, the deeper the coil is buried, the better the coil performs. However, for the northern part of the United States where the winter heating load is very high, the coil cannot be buried so deep that the ground temperature penetration in summer will not be enough to melt the soil frozen region built up through the whole winter season. A permafrost region around the coil could result. This model does not take into account the soil freezing effect. However, after a one-year simulation period with this model, a review of the ground temperature distribution should provide a good idea of whether a possible permafrost region around the coil has formed.

Conclusion

Ground coil design has long been dominated by line source theory. Most designers in this field are associated either with small contractors or with small consulting firms. They realize the drawbacks of using line source theory but lack the manpower and resources to perform a detailed mathematical analysis of the problem. This model, although it consumes more computer time, can now be used to check the ground coil design with other methods if it is not used for design purposes.

Notation

C = specific heat, J/kg · °C
DT = one-half amplitude of annual surface temperature, °C
h = convective heat transfer coefficient, W/m2 · °C
K = thermal conductivity W/m · h · °C
N_{Nu} = Nusselt number = $2hr_0/K_f$
N_{Re} = Reynolds number = $2Vr_0\rho_f/\mu$
r = radius, m
T = temperature, °C
TA = annual average ground surface temperature, °C
t = time, h
t_0 = time of the year, h
V = fluid velocity, m/h
x = distance along the ground coil, m
Z = depth, m

Greek letters

ρ = density, kg/m^3
θ = angular direction, Eq. 3
ϕ = phase angle, radian
α = thermal diffusivity = $K/\rho C_p$, m^2/h
μ = fluid viscosity, kg/(m · h)

Subscripts

0 = pipe inside wall
1 = pipe outside wall
f = fluid
i = initial
p = pipe
s = soil region
F = farfield

Literature cited

ASHRAE Handbook, 1981 Fundamentals, Am. Soc. Heating, Refrig., Air cond. Eng., pp. 18.3–18.8 (1981).
Coogan, C. H., Jr., "Heat Transfer Rate," *Mech. Eng.*, **26**, 495 (1949).

Donne, M. D., and F. H. Bowditch, "High-Temperature Heat Transfer." *Nucl. Eng.*, **8**, 20 (1963).

Freund, E. A., and G. S. Whitlow, "Earth-Source Heat Pumps: Characteristics, Design, and Operation," *J. Am. Inst. Electr. Eng.*, **540** (1959).

Ingersoll, L. R., F. T. Adler, H. J. Plass, and A. C. Ingersoll. "Theory of Earth Heat Exchangers for the Heat Pumps," *ASHVE Trans.*, **56**, 167 (1950).

Jacob, M., *Heat Transfer*, Wiley, New York, **1**, 549–550 (1958).

Johnson, S., B. McGraw, A. Bedinger, F. Conlin, and S. Wix, *Ground Coil Heat Pump, Interim Report No. 2 to Oak Ridge Nat. Lab.*, Energy, Environment and Resources Center, Univ. Tennessee, 76 (1983).

Kusuda, T., and P. R. Achenbach, "Earth Temperature and Thermal Diffusivity at Selected Stations in the United States, *ASHRAE Trans.*, **71**(1), 61 (1965).

Metz, P. D., *Ground-Coupled Heat Pump System Experimental Results*, Report BNL-33540, Brookhaven Nat. Lab. (1983).

Smith, G. S., "Factors Useful in Ground Grid Design for Heat Pumps," *ASHVE Trans.*, **56**, 189 (1950).

VDI-Warmeatlas, 3rd. ed., VDI-Verlag, Dusseldorf, Federal Republic of Germany, Sec. Gb, pp. 1–5 (1977).

Manuscript received Dec. 13, 1984, and revision received Dec. 26, 1985.